Journal of Chromatography A, 661 (1994) 227–238
Elsevier Science B.V., Amsterdam

CHROMSYMP. 2915

Quantitative polymer composition characterization with a liquid chromatography–Fourier transform infrared spectrometry–solvent-evaporation interface

T.C. Schunk*

Analytical Technology Division, Research Laboratories, Eastman Kodak Company, Rochester, NY 14650-2136 (USA)

S.T. Balke and P. Cheung

Department of Chemical Engineering and Applied Chemistry, University of Toronto, Toronto, Ontario M5S 1A4 (Canada)

ABSTRACT

Factors that are important to the quantitative analysis of polymer composition distribution by high-performance liquid chromatography (HPLC)–Fourier transform infrared (FT-IR) using a solvent-evaporation interface are investigated. These factors include the effects of the location and distribution of the deposited polymer films, as well as the morphology of the deposit. Consideration is given to the influence of these factors on the chromatographic resolution and FT-IR spectral quality. Size-exclusion separations of polystyrene and poly(methyl methacrylate) in tetrahydrofuran are used to demonstrate the impact of these effects on the quantitative use of the resulting FT-IR spectra. Results indicate that all absorbance bands are not uniformly affected by spectral distortions, but that compositional information can be obtained on simple blends. The effectiveness of a post-sample-collection solvent-annealing procedure is also considered.

INTRODUCTION

Size-exclusion chromatography (SEC) is well established for the characterization of molecular mass distributions of synthetic polymers. In addition to SEC, various forms of gradient high-performance liquid chromatography (HPLC) using adsorption, partition, precipitation, temperature-rising elution, and other "cross-fractionation" methods are being developed and applied to the characterization of synthetic polymer distributions other than molecular mass. These distributions include chemical composition, branching, stereochemistry, and end-group functionality [1,2]. Quantitative functional group-selective detection, such as Fourier transform infrared (FT-IR) spectrometry, is critical to the successful implementation of these fractionation methods.

The direct interfacing of HPLC and FT-IR has evolved from two directions: in-line flow cells and solvent evaporation prior to FT-IR spectral analysis. Low-volume flow cells offer continuous monitoring of the eluates with little loss of chromatographic resolution. Application has been limited, however, due to the strong infrared absorption inherent to HPLC eluents throughout much of the mid-infrared spectral range [3,4]. This interference also makes gradient elution HPLC impractical.

Solvent evaporation allows the use of the full

* Corresponding author.

0021-9673/94/$07.00
SSDI 0021-9673(93)E0882-U

mid-IR range without solvent spectral interference. Off-line FT-IR spectrometry can be performed with the advantage of increased sensitivity from unrestricted spectra signal averaging on samples that are in pure form with no diluting solvent. Solvent evaporation has gained favor recently over the flow-cell mode for both small molecule and polymer characterization [5–7].

HPLC–FT-IR detection of polymers using solvent evaporation has some commonality with small molecule detection. For example, several FT-IR optical configurations (transmission, external reflection, reflection-absorption, diffuse reflection, and diffuse transmittance) are possible after eluate deposition. A comparison by previous workers [8] for small-molecule spectroscopy indicates that conventional transmission FT-IR on flat subtrates yields the best information quality with the fewest spectral artifacts. There is no indication that small molecules and polymers differ significantly.

There are some important differences, however, between FT-IR detection using solvent evaporation for small molecules and polymers that are the focus of this study.

Resolution requirements. The emphasis of small-molecule analyses has been on minimum detectable quantity and minimum identifiable quantity [5] for well-resolved separations. However, quantitative polymer composition determination requires accurate representation of the entire polymer elution profile with minimum resolution loss. The term deposit distribution will be used to refer to the location of the eluates on the collection substrate relative to the infrared sampling beam. Deposit distribution is expected to be influenced by deposition conditions and instrumental configuration due to eluate remixing and deposit placement on the collection surface.

Deposited polymer morphology. A variety of spectral artifacts are possible when deposited eluates have size domains on the order of the wavelength of IR radiation [9]. Domains may be formed as a result of the deposition process and/or from eluate chemical effects. Considering that very few polymer blends are truly miscible on the molecular level, it is expected that morphological effects could be unique for polymeric materials. The term deposit morphology will be used to refer to domains within the polymer deposit on the scale of the infrared sampling wavelengths.

The above differences are generic to solvent evaporation interfaces and can be studied with a number of instrumental designs [9]. This investigation uses a commercial HPLC–FT-IR interface design based upon the work of Gagel and Biemann [10–12] and commercialized by Lab Connections Inc.

EXPERIMENTAL

The results described in this work were generated with an LC-Transform HPLC–FT-IR solvent evaporation interface manufactured by Lab Connections Inc. (Marlborough, MA, USA). The LC-Transform sample collection unit was connected to 55 p.s.i.g. N_2 gas supply (1 p.s.i.g. $= 69 \cdot 10^2$ Pa) and solvent vapors were removed by a 4-in. (*ca.* 10 cm) fume exhaust. Samples were collected on 60 mm diameter × 2 mm thick rear-surface-aluminized germanium (Ge–Al) disks throughout. Initial gas flow and temperature conditions were established by visually inspecting the film deposits from 0.5-μl direct injection of polymer samples. The nebulizer gas flow was set to 2.5 ml/min and the sheath gas to 4 l/min. The height of the nebulizer tip above the collection disk was left constant at 10 mm for all experiments (Fig. 1A). The flow-rate of eluent split to the sample collection unit (nominally 70 μl/min) was estimated by collecting several repeat measurements of a time aliquot of eluent and measuring its volume by drawing into a 100-μl graduate syringe.

The operational temperature range of the nebulizer was determined to be 35–40°C for tetrahydrofuran (THF) at 70 μl/min. Operation at a higher setting of 45°C caused the solvent to evaporate too early, producing clogging in the nebulizer. When the interface temperature was set too low (30°C), a visible amount of solvent was observed on the collection disk that interfered with the formation of a stable deposit.

Rotation of the collection disk was delayed for five minutes after sample injection and was then

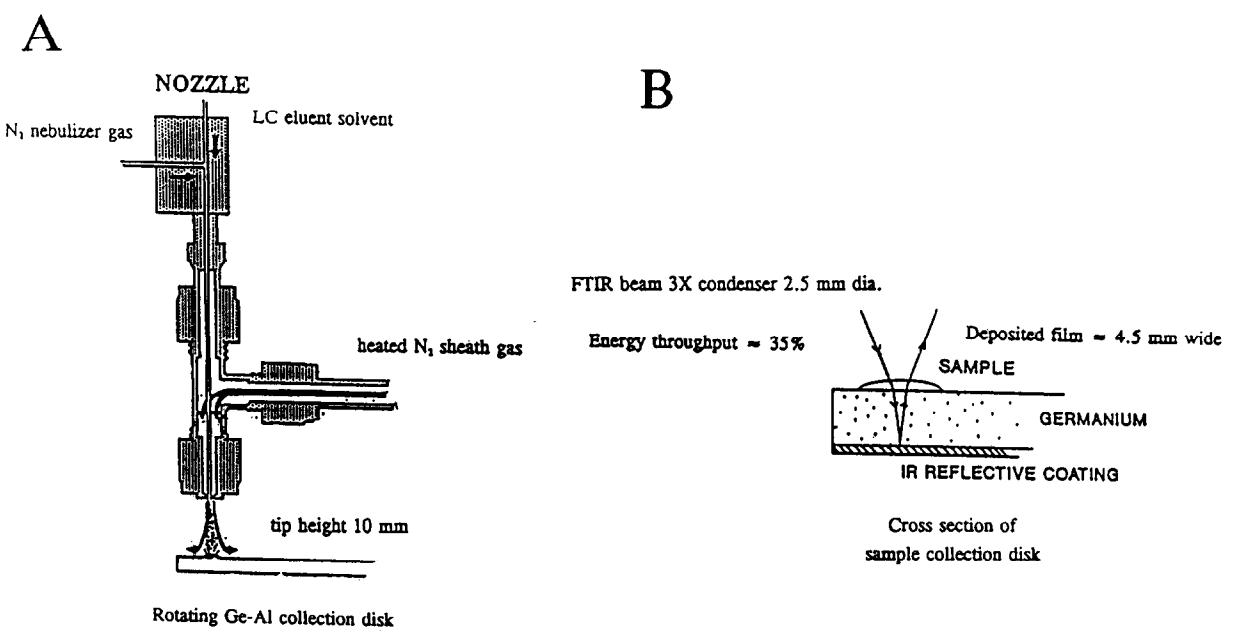

Fig. 1. (A) Diagram of the LC-Transform concentric flow nebulizer. (B) Ray diagram of the IR beam path through the sample deposit and rear-surface-aluminized-germanium collection disk.

rotated at 10°/min during polymer elution. This allowed up to five samples to be deposited on a single disk for the single SEC column separations. Disk rotation was delayed 15 min for three column separations. A disk rotation rate of 14.9°/min was used for the polystyrene (PS)–poly(methyl methacrylate) (PMMA) blend separation.

Separations were performed with a Perkin-Elmer (Norwalk, CT, USA) Series 4 HPLC operated at 1.0 ml/min. SEC separations were on either a single or three Polymer Laboratories (Amherst, MA, USA) PLgel 10-μm mixed bed 300×7.5 mm columns. Injections of 200-μl samples were made with a Perkin-Elmer ISS-100 autosampler. Each sample polymer solution was dissolved in THF containing 0.06% (v/v) toluene as a UV-absorbing flow marker. Sample concentrations were 1.0, 3.0, or 6.0 mg/ml for PS, 3.0 mg/ml for PMMA, and 1.5 mg/ml each for the PS–PMMA blend. THF eluent was redistilled from CaH_2 prior to use and was sparged with helium during use. PS NBS 706 was obtained from NIST (Washington, DC, USA) and PMMA broad standard 037B was obtained from Scientific Polymer Products, (Ontario, NY, USA). PS elution profiles were monitored by a Kratos Model 773 (Ramsey, NJ, USA) UV absorbance detector at 270 nm directly after the SEC column(s) and before the solvent flow divider. PMMA elution profiles were determined separately with a Waters Assoc., Division of Millipore (Milford, MA, USA) Model R401 differential refractive index (DRI) detector.

After polymer sample deposition, the Ge–Al collection disk was manually transferred to the FT-IR scanning module and a series of spectra collected while rotating the disk under the IR beam. FT-IR spectra were obtained on a dry-nitrogen-purged Nicolet 20SXB (Madison, WI, USA) spectrometer with the LC-Transform scanning module aligned in the sample chamber. A ray diagram of the optical path of the 2.5-mm IR beam through the sample deposit on the Ge–Al disk is shown in Fig. 1B. FT-IR spectra at 8 cm^{-1} resolution were collected by averaging 8 scans while the disk was rotated at 5°/min. A disk rotation rate of 10°/min was used for PS and PS–PMMA blend samples separated on three SEC columns.

Optical microcopy of the deposited polymer films on the Ge–Al collection disks was per-

formed with a Jenatech (Germany) binocular inspection microscope equipped with a Hitachi (Japan) VK-C360 color video camera. Micro-FT-IR spectrometry of selected polymer deposits was performed on a Digilab FTS60 FTIR spectrometer with a UMA 300A IR microscope in reflectance mode with a 10 μm beam diameter in 100-μm steps at 8 cm^{-1} resolution from 512 scans.

RESULTS AND DISCUSSIONS

Chromatographic resolution

Size-exclusion chromatography (SEC) separations of broad polymer standards were employed as model separations for the investigation of quantitative polymer FT-IR detection. Chromatographic peak dispersion associated with the solvent-evaporation interface was evaluated by comparing the polymer concentration elution profile as determined with an in-line detector (UV or DRI) with that reconstructed from the FT-IR data (FT-IR chromatogram). FT-IR and concentration chromatograms were aligned based upon their chromatographic peak maxima. The assumption of a linear Beer's law relationship between sample mass and FT-IR response area was made in plotting FT-IR chromatograms. This needs to be experimentally verified for the instrumental configuration employed.

The resolution loss for an FT-IR chromatogram of PS produced from the integrated intensity of the phenyl absorbance band at 698 cm^{-1} is shown in Fig. 2. Direct comparison can be made to the concentration chromatogram determined by a UV absorbance detector. A simple comparison of the peak base width from extrapolated inflection points gives a variance ratio of 1.36 FTIR:UV chromatograms (assuming an approximately Gaussian profile, base width = 4σ).

Aside from any dispersion effects in the connecting tubing leading to the interface nebulizer, two band-broadening effects should be specific to the deposition and sampling method employed. The finite diameter of the nebulized eluent spray impinging on the collection disk surface leads to the deposition of polymer over a specific area. As the collection disk is moved past this position, additional material must be laid down in the overlap region leading to some remixing and resolution loss. In addition, during FT-IR spectra collection the diameter of the IR beam sampling the eluate deposit has the effect of providing a spectrum which is a time average of a region of the sample deposit. This would also result in an effective resolution loss. These effects, however, could be altered by choice of the disk rotation rate and FT-IR spectral sampling time. In addition, compensation for both of these effects would assume that there is no sample-dependent effect on deposit distribution on the collection disk surface.

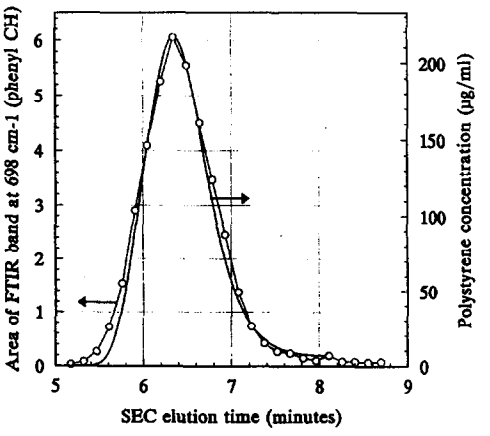

Fig. 2. SEC chromatograms of a 1.00 mg/ml polystyrene NBS 706 200-μl injection separation on one PLgel 10-μm mixed bed column at 1.0 ml/min THF, split flow 74 μl/min. Concentration chromatogram from the UV absorbance response at 270 nm (line). FT-IR chromatogram from the integrated area of the absorbance band at 698 cm^{-1} (data points) from the Ge–Al deposited sample.

Significantly different resolution loss behavior was observed, however, for a broad PMMA sample. An overlay plot of the PMMA SEC concentration chromatogram determined with an in-line DRI detector and the FT-IR chromatogram determined from the absorbance band area of the 1730 cm^{-1} carbonyl band is shown in Fig. 3. Surprisingly, the FT-IR chromatogram of PMMA is more narrow than the DRI concentration elution profile. This behavior may be explained by observation of the distribution of the deposited polymer film. The uppermost deposit on the Ge–Al disk in the photograph of Fig. 4 is the PMMA sample used to generate the

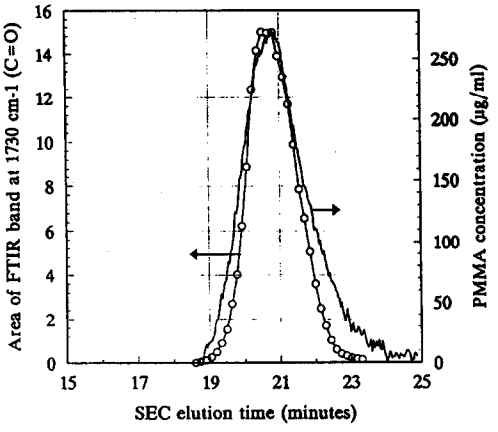

Fig. 3. SEC chromatograms of a 3.00 mg/ml poly(methyl methacrylate) 200-μl injection separation on three PLgel 10-μm mixed bed columns at 1.0 ml/min THF, split flow 103 μl/min. Concentration chromatogram from the DRI detector response (line). FT-IR chromatogram from the integrated area of the absorbance band at 1730 cm^{-1} (data points) from the Ge–Al deposited sample.

data of Figs. 3 and 5. Note that, although the deposited polymer stripe increases in width gradually at the beginning of deposition, the trailing portion of the deposit is split into two tails. At the tails of the polymer deposit a large percentage of the sample lies outside the 2.5 mm

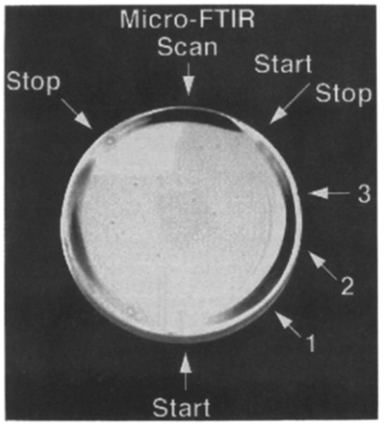

Fig. 4. Photograph of three polymer sample deposits on a Ge–Al collection disk. The upper deposit stripe is the PMMA sample described in Figs. 3, 5, 10, and 11. The right deposit stripe is the PS–PMMA blend sample described in Figs. 13–17. The arrows numbered 1, 2, and 3 correspond to the optical microscopy images of Fig. 17. Increasing elution time is counterclockwise.

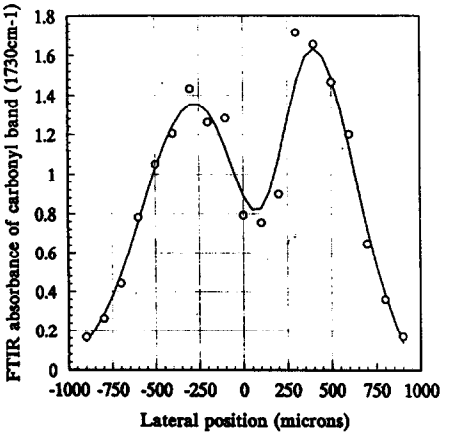

Fig. 5. Micro-FT-IR profile of the PMMA deposit location marked in Fig. 4. The IR beam diameter was 10 μm with 100-μm steps and 512 scans averaged at 8 cm^{-1} resolution.

IR beam diameter producing the erroneously narrow SEC profile described in Fig. 3. This deposit distribution is attributable to displacement of the wet film by the nebulizer gas jet during deposition and was confirmed to be present across the entire PMMA deposit by micro-FT-IR as shown in Fig. 5. This effect of analyte spot "washout" has also been described by Fraser *et al.* [13] and emphasizes the need for matching IR sampling beam diameter to analyte deposit width. From current data it cannot be determined whether this effect is due primarily to deposition conditions or has contributions from sample composition.

Spectral quality

The morphology of the deposited polymer can be investigated by optical microscopy. An example of the appearance of a polystyrene film is shown in Fig. 6. A wide range of particles are present in the film. Many of the larger particles have run together to form chains. It can be estimated from deposition conditions that the thickness of the deposited polymer corresponding to the SEC peak maximum is approximately 1.2 μm for a 1.00 mg/ml PS injection. In relation to the observed size of the deposited polymer features, it is not clear whether the irregular polymer morphology results from the nebulizer droplet evaporation or has contributions from interfacial tension between the hydro-

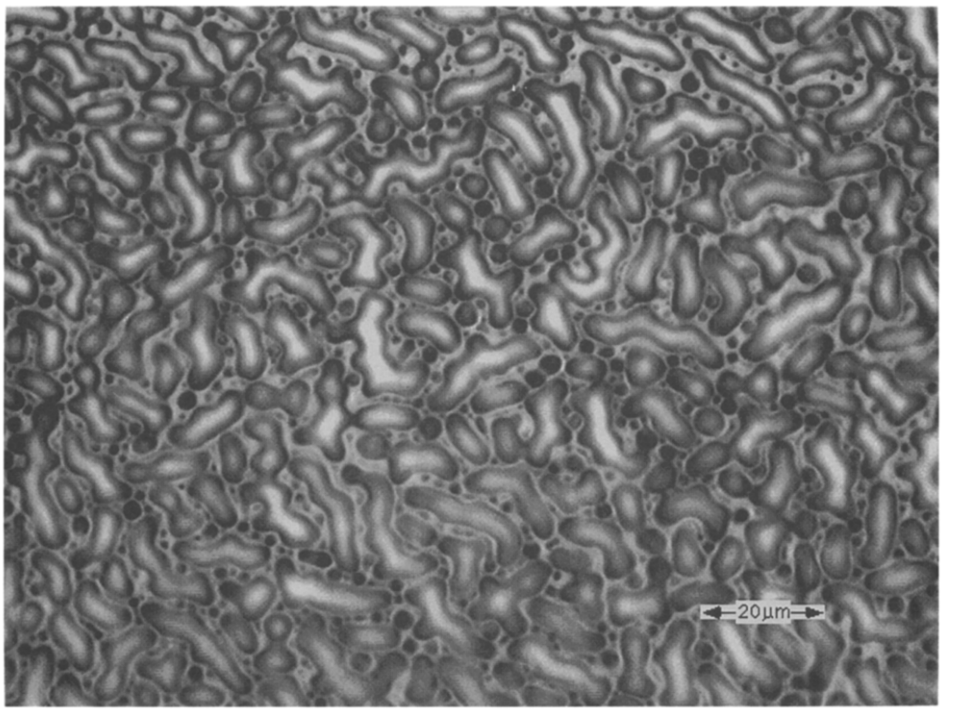

Fig. 6. Optical microscopy image of the deposit morphology of the polystyrene NBS 706 sample on the Ge-Al collection disk corresponding to Figs. 2, 7, and 8.

phobic polystyrene and the hydrophilic germanium surface.

A typical FT-IR spectrum of the deposited polystyrene film is shown in the upper trace of Fig. 7 obtained near the SEC peak maximum. A prominent feature of all the PS spectra collected was the large sloping background superimposed with the IR absorbance bands. This background is characteristic of the scattering of the IR radiation by the sample deposit. The range of particles sizes observed in Fig. 6 is consistent with the scattering observed in the mid-infrared wavelength range of 2.5 to 20 μm.

The intensity of the background scattering at 3600 cm^{-1} due to the irregular structure of the deposited PS follows the PS concentration profile as shown in Fig. 8. A correlation between polymer concentration and background scattering was observed for all PS-containing samples.

In an attempt to improve the quality of the FT-IR spectra obtained from the PS deposit, a solvent annealing procedure was used. The sample-containing disk was briefly exposed to the vapor above boiling dichloromethane. The visible appearance of the polymer deposit on the disk changed from a matte finish to a clear film showing visible light interference fringes. Low-

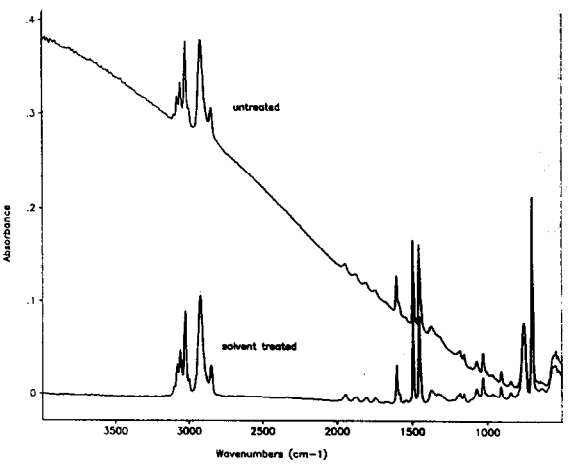

Fig. 7. Overlay FT-IR spectra of the polystyrene NBS 706 deposit corresponding to Figs. 2, 6, 8, and 9, before (upper trace) and after (lower trace) dichloromethane vapor annealing. FT-IR 8 scans, 8 cm^{-1} resolution.

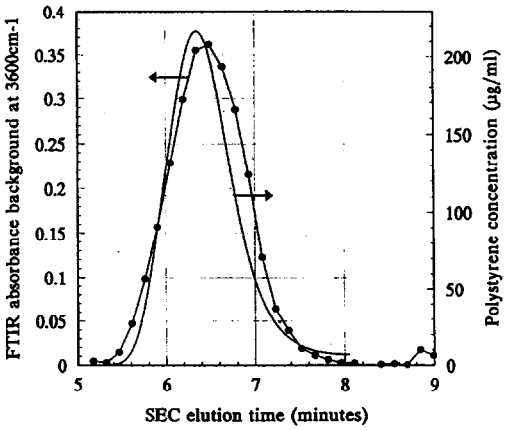

Fig. 8. SEC chromatogram of the same sample shown in Figs. 2 and 6. Comparison of the concentration chromatogram from the UV absorbance response at 270 nm (line) and the FT-IR background scattering intensity at 3600 cm^{-1} (data points).

power magnification of the leading edge of the polymer deposit after solvent annealing is shown in Fig. 9. The film became discontinuous at the edge, showing many large (>100 μm) domains. The gradation in the continuous film at the left of the image appears as colored interference fringes in visible light. The irregularity and fingering at the edges of the polymer domains is again indicative of some contribution of high interfacial tension to the structure of the PS film of the germanium surface.

The lower trace of Fig. 7 shows the FT-IR spectrum of the deposited PS film after solvent treatment. The absorbance bands are of similar intensity before and after solvent treatment, but the scattering background is absent after annealing. The FT-IR chromatogram of the PS deposit after solvent annealing showed little difference relative to the original deposit with the exception of a small decrease in SEC peak maximum response. Unfortunately, the manual annealing procedure was difficult to reproduce and it would be preferable to avoid the complexity of post-sample-collection treatments which could easily lead to chromatographic resolution loss.

The effect of polymer composition on deposit morphology is demonstrated by the appearance

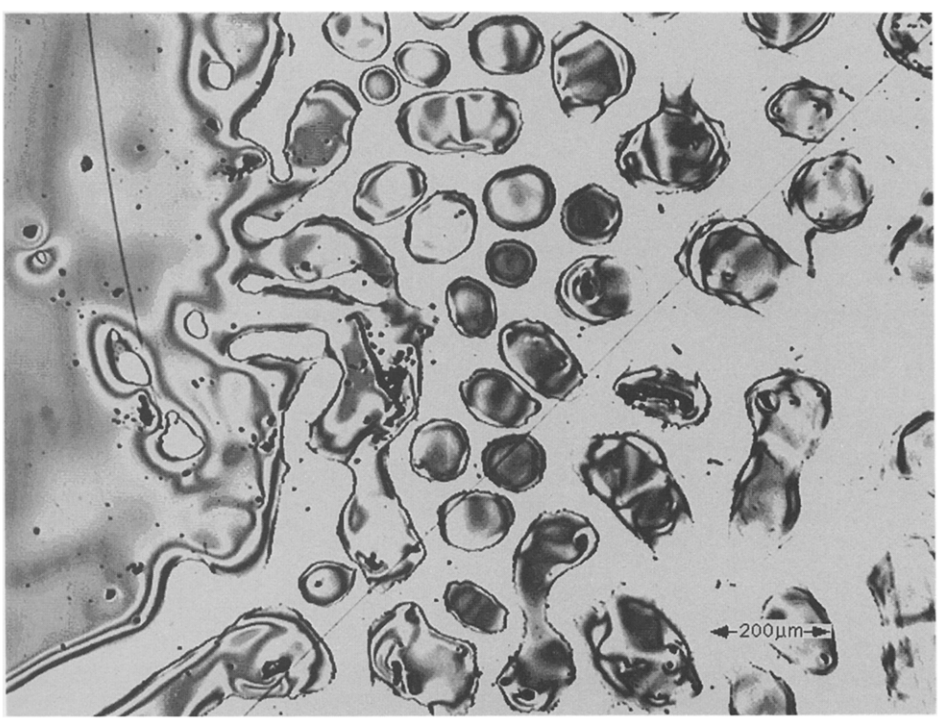

Fig. 9. Optical microscopy image of the dichloromethane vapor annealed polystyrene NBS 706 deposit corresponding to the lower trace of Fig. 7.

of the PMMA sample deposit. Optical microscopy of the PMMA film morphology gave the appearance of a random arrangement of irregular plates (Fig. 10). The FT-IR spectra of the PMMA film deposited on the Ge–Al disk (Fig. 11) did not show the scattering distortions associated with the PS samples.

The quality of the IR spectra and their utility for reconstructing SEC–FT-IR chromatograms was investigated by comparing FT-IR chromatograms from three characteristic IR absorbance bands for a three-column SEC separation of PS (Fig. 12). Band intensities were measured relative to local spectral baselines and were normalized based on the SEC response maximum. Some relative shifts in the SEC profiles described by the different bands can be noted, particularly on the high-retention side of the polymer distribution. The shorter wavelength bands do not show as good an agreement with the UV profile as does the strong 698 cm^{-1} band.

Band ratios across each SEC elution profile between SEC peak half height points were calculated as shown in Table I for comparison of the spectral quality. To investigate the possible effects of solid-state interactions and scattering distortions, the ratio of two different bands (3080 and 698 cm^{-1}) were calculated relative to the C–C band at 1600 cm^{-1}. The 698/1600 cm^{-1}

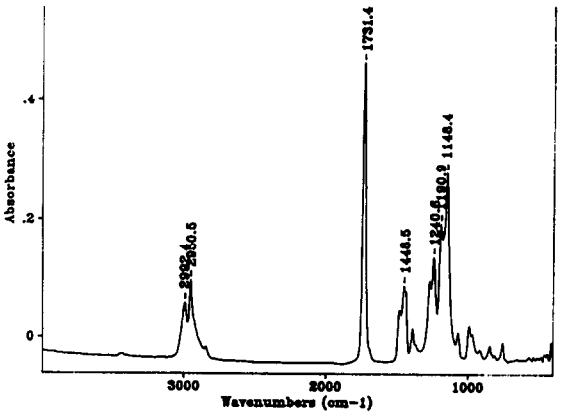

Fig. 11. FT-IR spectrum from 8 scans at 8 cm^{-1} resolution of the PMMA deposit corresponding to Fig. 10 near the maximum of the SEC chromatogram of Fig. 3.

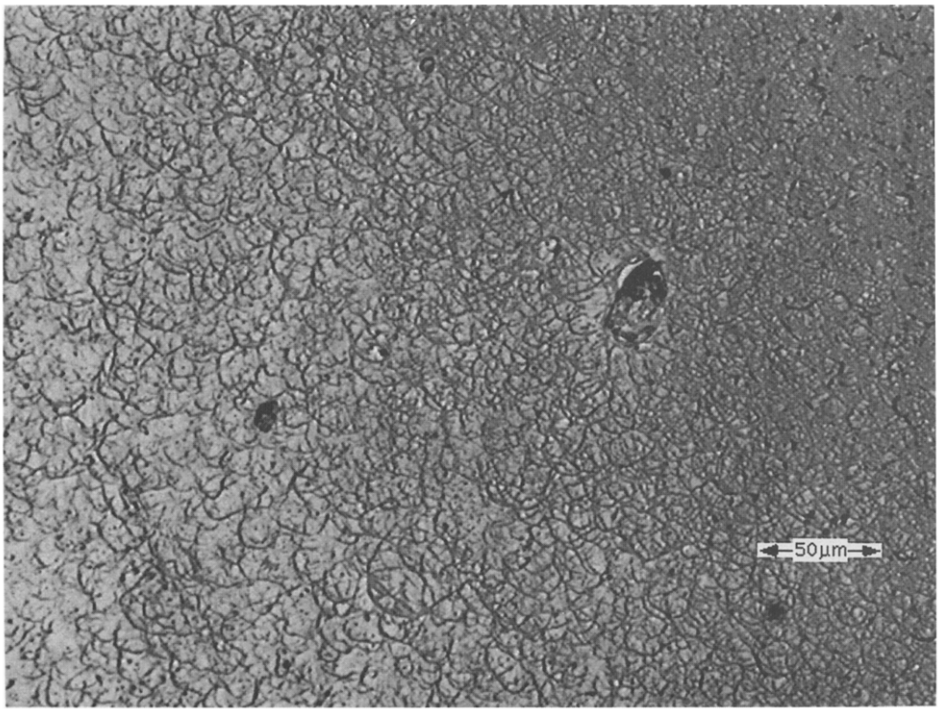

Fig. 10. Optical microscopy image of the morphology of the PMMA deposit on the Ge–Al collection disk corresponding to Figs. 3–5.

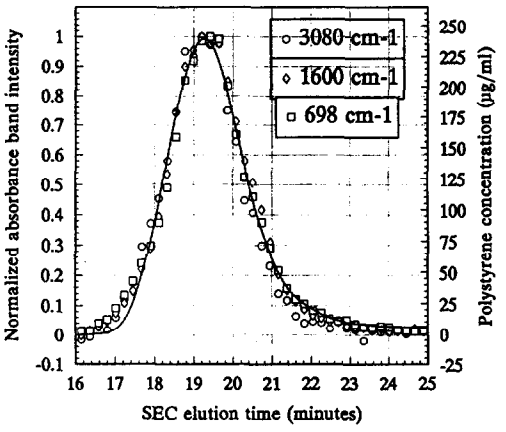

Fig. 12. SEC chromatograms of a 3.00 mg/ml PS NBS 706 200-μl injection separation on three PLgel 10-μm mixed bed columns at 1.0 ml/min THF, split flow 72 μl/min. Concentration chromatogram from the UV absorbance response at 270 nm (line). Data points represent the absorbance intensity of the FT-IR bands at 3080 (○), 1600 (◇), and 698 cm^{-1} (□) obtained from the Ge–Al disk-deposited sample.

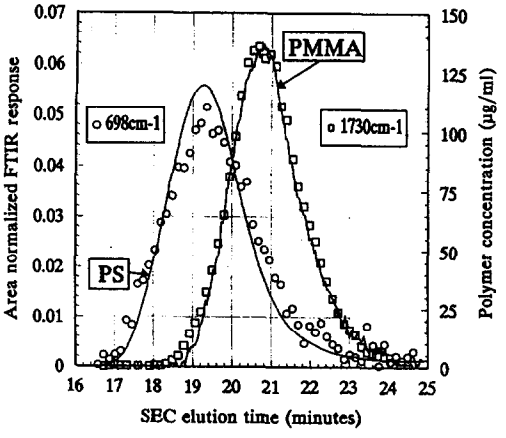

Fig. 13. SEC chromatograms of 1.5 mg/ml each PMMA (DRI response) and PS NBS 706 (UV absorbance 270 nm response) (lines) 200-μl injections on three PLgel 10-μm mixed bed columns at 1.0 ml/min THF measured separately. Data points represent the integrated area of the FT-IR absorbance bands at 698 (○) and 1730 cm^{-1} (□) obtained from a Ge–Al disk-deposited blend sample of these polymers with split flow at 94 μl/min and corresponding to Fig. 4.

ratio was relatively constant for all of the samples. Considerable variability was seen with the 3080/1600 cm^{-1} ratio, particularly for the samples before and after solvent annealing. This observation emphasizes the spectral distortions associated with the scattering of the IR radiation by the irregular deposit morphology.

Compositional distribution determination

Of most interest in the application of an HPLC–FT-IR solvent-evaporation interface is the determination of the variation in chemical composition across a polymer chromatogram. SEC separation of a blend of a broad PMMA and NBS 706 PS was used to investigate the capabilities for the determination of accurate polymer composition profiles.

The FT-IR chromatograms of the PS (698 cm^{-1} band) and PMMA (1730 cm^{-1} band) components of the blend are compared to the corresponding in-line detector concentration chromatograms in Fig. 13. The FT-IR chromatograms of PS and PMMA were normalized by SEC peak area for the uncalibrated concentration response. Although the chromatogram profiles agree fairly well, it is apparent that the PS profile shows more resolution loss than that of PMMA. The composition profile of the PS–

TABLE I

SAMPLE EFFECT ON FT-IR ABSORBANCE BAND RATIOS

Sample	3080/1600 cm^{-1}	S.D.	698/1600 cm^{-1}	S.D.
3.0 mg/ml PS	0.708	0.043 ($n = 9$)	5.02	0.22 ($n = 9$)
1.0 mg/ml PS	0.533	0.065 ($n = 7$)	4.83	0.19 ($n = 7$)
DCM[a] annealed 1.0 mg/ml PS	1.01	0.12 ($n = 7$)	4.76	0.43 ($n = 7$)
PS–PMMA blend	0.728	0.098 ($n = 18$)	4.79	0.39 ($n = 18$)

[a] DCM = dichloromethane.

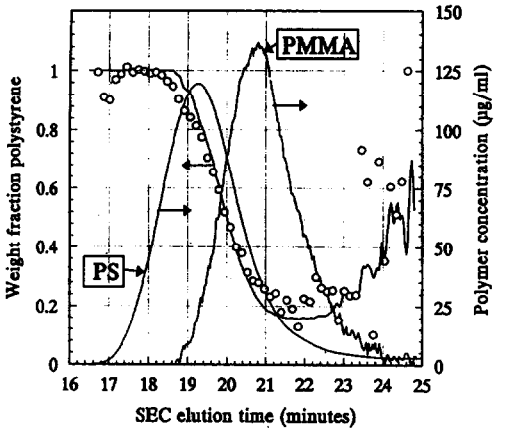

Fig. 14. SEC concentration chromatograms as described in Fig. 13. Comparison of the calculated weight fraction of PS from the concentration profiles (line) and from the FT-IR chromatogram data of Fig. 13 (data points).

PMMA blend was calculated as % (w/w) PS in Fig. 14 and compared to the UV and DRI concentration profiles. The FT-IR-determined blend composition is reasonably accurate in the middle of the chromatogram, but accuracy decreases in the wings of the chromatogram. It has not been determined which deposit distribution or morphological variations contribute most to the broadening of the PS portion of the FT-IR chromatogram.

Fig. 15 shows the FT-IR spectrum obtained near the middle of the blend chromatogram.

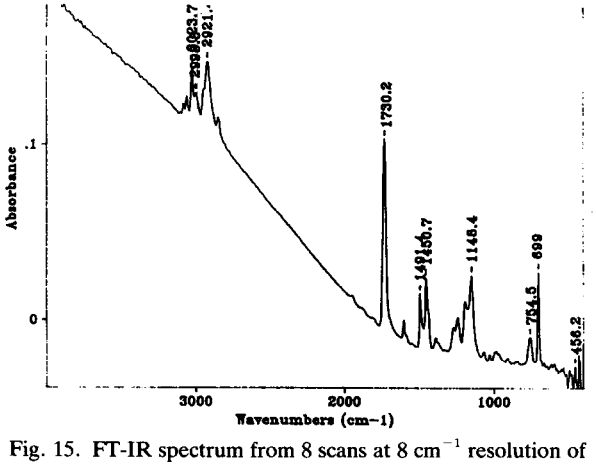

Fig. 15. FT-IR spectrum from 8 scans at 8 cm^{-1} resolution of the PS–PMMA blend deposit corresponding to Figs. 4, 13, and 14 obtained near the maximum of the SEC chromatogram (arrow position 2 on Fig. 4).

Note that the scattering background diminishes with increasing wavelength more rapidly than was observed for a pure PS deposit (Fig. 7). The presence of PMMA mixed with PS apparently produces fewer large scattering features than were present in a pure PS deposit.

The absorbance signal at 3600 cm^{-1} was used to map the background scattering intensity across the FT-IR chromatogram. Fig. 16 shows these data points in comparison to the spline fit smoothed FT-IR chromatograms at 698 cm^{-1} (PS) and 1730 cm^{-1} (PMMA). There is a clear correspondence between the scattering background intensity and the relative PS concentration.

A minimum in the scattering intensity occurs at the PMMA response maximum. This spectral response is consistent with the morphology of the polymer deposit as observed by optical microscopy. The optical micrographs of three locations on the blend deposit are shown in Fig. 17. Fig. 17A is quite similar to the morphology seen in Fig. 6 for a pure PS deposit. Fig. 17C appears similar to deposits observed for pure PMMA and Fig. 17B is intermediate.

Distortions present in the FT-IR spectra of the PS–PMMA blend were also evaluated by absorbance band ratios (Table I). There is reasonable agreement with values obtained from the pure PS deposit spectra. There are no obvious band-intensity distortions associated with the

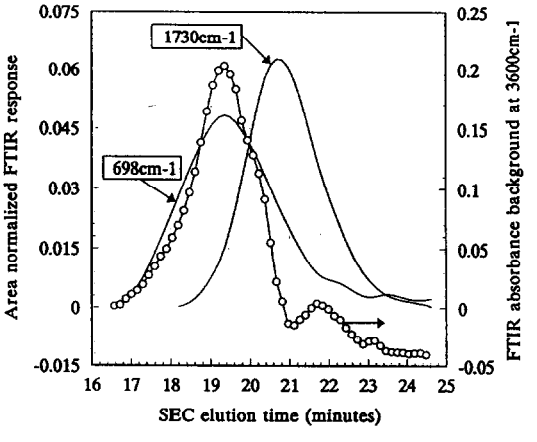

Fig. 16. Spline fit smoothed FT-IR chromatograms of the data points shown in Fig. 13. Comparison to the FT-IR scattering background intensity at 3600 cm^{-1} (data points).

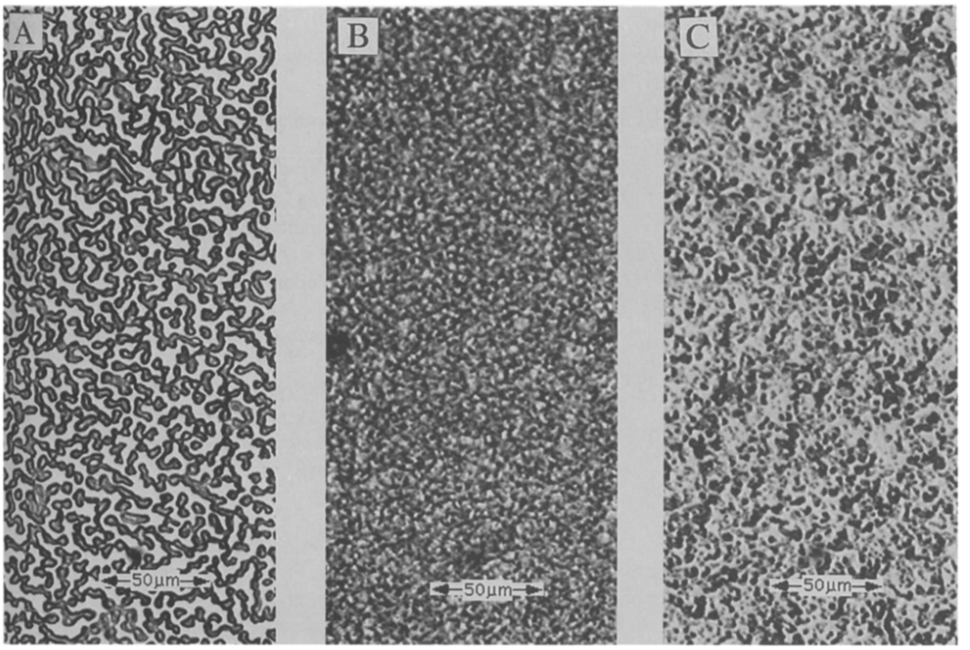

Fig. 17. Optical microscopy image of the morphology of the PS–PMMA blend deposit corresponding to the arrow positions of Fig. 4. (A) PS rich region at arrow position 1, (B) blend region at arrow position 2 (spectrum Fig. 15), and (C) the PMMA rich region at arrow position 3.

presence of PMMA blended with the PS in the deposit other than those due to scattering.

CONCLUSIONS

Several points for further investigation and performance improvements have been identified by the experimental evaluations described which are in general agreement with the findings of other researchers evaluating small molecule applications [5,8,13].

The novel FT-IR sampling configuration of transmission-reflection on a rear-surface-aluminized germanium disk was found to provide good signal-to-noise IR spectra which resembled conventional transmission spectra.

Lateral variations in polymer deposit distribution, particularly for sample "washout" from the center of the deposit, can result in significant chromatographic resolution distortions. This emphasizes the need to accurately match the deposit width with the IR beam diameter.

Irregular morphology of the deposited polymer films associated with a wide size distribution of features can produce intense IR-scattering backgrounds superimposed on the absorbance spectra.

Relative changes in IR band intensities accompany the IR-scattering effects, thus complicating quantitation.

Limited success with solvent annealing showed the elimination of the IR-scattering background, but was difficult to control experimentally and can lead to severe resolution distortion.

The determination of accurate composition profiles from the FT-IR spectral data of sample deposits relies on the maintenance of the chromatographic resolution. Reasonable compositional accuracy was found near the center of SEC distributions with increasing error at the wings.

ACKNOWLEDGEMENTS

Assistance in these experimental evaluations is gratefully acknowledged from J. Willis and J. Dwyer (Lab Connections Inc.) for interface operation; T.H. Mourey for manuscript im-

provements; L.E. Oppenheimer for optical microscopy; W.P. McKenna, S.A. Yeboah, and D. Margevich for FT-IR spectrometry, and S. Markel for micro-FT-IR spectrometry (all of Eastman Kodak Company).

REFERENCES

1 T.H. Mourey and T.C. Schunk, in E. Heftmann (Editor), *Chromatography*, (*J. Chromatogr. Library*, Vol. 51B), Elsevier, Amsterdam, 5th ed., 1992, pp. 475–512.
2 T.C. Schunk, *J. Chromatogr. A*, 656 (1993) 591.
3 C.W. Saunders and L.T. Taylor, *Appl. Spectrosc.*, 45 (1991) 900.
4 K. Nishikida, T. Housaki, M. Morimoto and T. Kinoshita, *J. Chromatogr.*, 517 (1990) 209.
5 A.J. Lange, P.R. Griffiths and D.J.J. Faser, *Anal. Chem.*, 63 (1991) 782.
6 A.H. Dekmezian, T. Morioka and C.E. Camp, *J. Polym. Sci.: Part B: Polym. Phys.*, 28 (1990) 1903.
7 A.H. Dekmezian and T. Morioka, *Anal. Chem.*, 61 (1989) 458.
8 R. Fuoco, S.L. Pentoney, and P.R. Griffiths, *Anal. Chem.*, 61 (1989) 2212.
9 P. Cheung, S.T. Balke, T.C. Schunk and T.H. Mourey, *J. Appl. Polym. Sci., Symp. Ed.*, in press.
10 J.J. Gagel and K. Biemann, *Anal. Chem.*, 58 (1986) 2184.
11 J.J. Gagel and K. Biemann, *Anal. Chem.*, 59 (1987) 1266.
12 J.J. Gagel and K. Biemann, *Mikrochim. Acta*, 11 (1988) 185.
13 D.J.J. Fraser, K.L. Norton and P.R. Griffths, in R.G. Messerschmidt and M.A. Harthcock (Editors) *Infrared Microspectroscopy: Theory and Applications*, Marcel Dekker, New York, 1988, pp. 197–210.